JVI Accepts, published online ahead of print on 19 March 2014
J. Virol. doi:10.1128/JVI.03801-13

Protein ISGylation delays but does not overcome coronavirus proliferation in a model of fulminant hepatitis

Xue-Zhong Ma[1], Agata Bartczak[1], Jianhua Zhang[1], Wei He[1], Itay Shalev[1], David Smil[2], Limin Chen[1], Jim Phillips[1], Jordan J. Feld[3], Nazia Selzner[1], Gary Levy[1], Ian McGilvray[1]#

Multi-Organ Transplant Program, University Health Network, University of Toronto, Toronto, Ontario, Canada[1]; Structural Genomics Consortium, University of Toronto, Toronto, Ontario, Canada[2]; Toronto Centre for Liver Disease, McLaughlin-Rotman Centre for Global Health, University of Toronto, Toronto, Canada[3].

Short Title: ISGylation is antiviral to Coronavirus

Word Count: Abstract (235); Article (5,600)

#Ian D McGilvray
11C1250 NCSB Toronto General Hospital
585 University Avenue
Toronto, Ontario M5G 2N2
Phone: 416 340 5230
Fax: 416 340 5242
Email: ian.mcgilvray@uhn.ca
Xue-Zhong Ma and Agata Bartczak contributed equally to this work

25 **Abstract**

26 Coronaviruses express a de-ubiquitinating protein, the papain-like protease-2 (PLP2), that re-
27 moves both ubiquitin and the ubiquitin-like Interferon (IFN) Stimulated Gene 15 (ISG15) protein
28 from target proteins. ISG15 has antiviral activity against a number of viruses therefore, we exam-
29 ined the effect of ISG15 conjugation (ISGylation) in a model of acute viral hepatitis induced by
30 the murine hepatitis virus (MHV)-3 coronavirus. Mice deficient in the ISG15 deconjugating en-
31 zyme, ubiquitin specific peptidase-18 (USP18), accumulate high levels of ISG15-conjugated pro-
32 teins and are hypersensitive to type I IFN. Infecting USP18$^{-/-}$ mice with MHV-3 resulted in ex-
33 tended survival (8 ± 1.2 vs. 4 days), and improved liver histology, a decreased inflammatory re-
34 sponse, and 1-2 logs lower viral titers compared to USP18$^{+/+}$ mice. The suppression of viral rep-
35 lication was not due to increased IFN, since infected USP18$^{-/-}$ mice had neither increased hepatic
36 IFN-α, -β or -γ mRNA nor circulating protein. Instead, delayed MHV-3 replication coincided
37 with high levels of cellular ISGylation. Decreasing ISGylation by knockdown of the ISG15 E1
38 enzyme, Ube1L, in primary USP18$^{+/+}$ and USP18$^{-/-}$ hepatocytes led to increased MHV-3 replica-
39 tion. Both *in vitro* and *in vivo*, increasing MHV-3 titers were coincident with increased PLP2
40 mRNA and decreased ISGylation over the course of infection. The pharmacologic inhibition of
41 the PLP2 enzyme *in vitro* led to decreased MHV-3 replication. Overall, these results demonstrate
42 the antiviral effect of ISGylation in an *in vivo* model of coronavirus-induced mouse hepatitis and
43 illustrate that PLP2 manipulates the host innate immune response through the ISG15/USP18
44 pathway.

45 **Statement of Importance**

46 There have been a number of serious worldwide pandemics due to widespread infections by
47 Coronavirus. This virus (in its many forms) is difficult to treat, in part because it is very good at
48 finding "holes" in the way that the host (the infected individual) tries to control and eliminate the
49 virus. In this study we demonstrate that an important host viral defence - the ISG15 pathway - is
50 only partially effective in controlling severe Coronavirus infection. Activation of the pathway is
51 very good at suppressing viral production, but over time the virus overwhelms the host response
52 and the effects of the ISG15 pathway. This data provides insight into the host-viral interactions
53 during Coronavirus infection and suggests that the ISG15 pathway is a reasonable target for con-
54 trolling severe Coronavirus infection, though the best treatment will likely involve multiple
55 pathways and targets.
56

57 **Introduction**

58 Coronaviruses cause both common and severe clinical illness, as manifested by the Se-
59 vere Acute Respiratory Syndrome (SARS) epidemic. During the 2002-2003 SARS epidemic,
60 8422 people were affected of whom 916 died from acute respiratory distress syndrome (1, 2).
61 The episodic re-emergence of severe coronavirus infections, most recently in the fall of 2012 and
62 continuing into 2013 highlights the need for treatments against Coronavirus infections (3).

63 Coronaviruses are positive stranded enveloped RNA viruses with some of the largest vi-
64 ral genomes ranging between 26-32kDa. Coronaviruses target a myriad of distinct animal hosts
65 and cause disease in a number of organs such as the brain, liver and lung. Organ damage from
66 severe coronavirus infections is generally the result of an over-exuberant activation of host in-
67 nate immune mechanisms (4, 5). For example, Murine Hepatitis strain-3 (MHV-3) infection of
68 susceptible mouse strains is a model of strong innate immune activation, resulting in fulminant
69 viral hepatitis (6). Following infection by MHV-3, mice die in 3-4 days of hepatic parenchymal
70 destruction mediated by a robust activation of local innate immunity (7-9). Understanding the
71 limits of host immunity in the MHV-3 model may identify novel targets for the treatment of se-
72 vere Coronavirus infections.

73 Interferon (IFN) stimulation as well as bacterial and viral infection induces the expression
74 of IFN stimulated genes (ISGs). One of the most abundantly expressed ISGs is ISG15, a 15-kDa
75 protein (10). ISG15 is conjugated to target proteins, the process of ISGylation, through consecu-
76 tive interactions with an E1 activating enzyme (Ube1L), an E2 conjugating enzyme (UbcH6 or
77 UbcH8) and an E3 ligase (Herc5, EFP, HHARI) (11). Over 160 proteins have been identified as
78 targets of ISG15 including proteins involved in processes such as protein translation, cell cycle
79 regulation and immune regulation (11-13). Several ISG15 downstream targets are involved in the

80 regulation of IFN signalling, including retinoic acid-inducible gene 1 (RIG-1), signal transducer
81 and activator of transcription -1 (STAT-1), janus activated kinase-1 (JAK-1) and MxA (12-14).
82 Although the ISG15 protease function has the potential to modulate IFN responses, this role has
83 not been consistently demonstrated (15). The effect of ISGylation on downstream proteins is
84 multifaceted as ISGylation has been reported to disrupt target protein function and/or alter cellu-
85 lar localization (16, 17).

86 The conjugation of ISG15 to protein targets is offset by the deconjugating activity of the
87 ubiquitin specific peptidase-18 (USP18). USP18, like ISG15, is an ISG, which is up-regulated
88 after stimulation by IFN, or by viral and bacterial infection. USP18 is specific for ISG15 and
89 strips ISG15 from target proteins through its isopeptidase activity (18). USP18$^{-/-}$ mice have
90 markedly increased cellular ISGylation, and are hyper-sensitive to the effects of Type 1 IFN (19-
91 21). The latter effect is independent of the isopeptidase activity, and instead due to the ability of
92 USP18 to modulate IFN signalling by binding to the IFNα receptor 2 (IFNAR2) (22). Thus,
93 USP18 has several functions important to the host innate immune response: by binding to the
94 IFNAR2 it can modulate the IFN response; and, through its ISG15 isopeptidase function it regu-
95 lates the cellular ISGylation levels. However the implications of the balance of ISGylation and
96 USP18 isopeptidase activity require further elucidation.

97 The role of ISGylation in viral lifecycles is specific to the virus involved. ISGylation can
98 exert an antiviral pressure against some infections, but can also stimulate viral replication in oth-
99 ers. For example, USP18 deficient mice have increased ISGylation and are more resistant to
100 lymphocytic choriomeningitis virus (LCMV) and herpes simplex virus (HSV) models of fatal
101 viral encephalitis (20). During human immunodeficiency virus (HIV) infection the conjugation
102 of ISG15 to the HIV Gag protein arrests assembly of the Gag particle on the plasma membrane

103 (23), and inhibits viral replication. On the other hand, we have found that ISGylation is necessary
104 for robust production of HCV in human hepatocytes (24), and both ISG15 and USP18 are up-
105 regulated in the hepatocytes of patients with chronic HCV who do not respond to exogenous IFN
106 treatment (25-27).

107 Previously, we demonstrated that coronavirus replication *in vivo* is held in check by host
108 ubiquitination (28). Inhibition of the cellular proteasome leads to increased cellular ubiquitina-
109 tion levels and an early interruption in coronavirus replication. Coronaviruses have evolved
110 counter-measures to such host cellular antiviral mechanisms. In this case, the de-ubiquitination
111 protein papain-like protease-2 (PLP2) strips ubiquitin from target proteins (29). The PLP2 pro-
112 tein is not specific to ubiquitin: it acts on both ubiquitin and the ubiquitin-like protein, ISG15.
113 This suggests that ISG15 and its conjugation to cellular proteins may also exert an antiviral pres-
114 sure effect against coronavirus infection. Moreover, several reports indicate that PLP2 has a 60-
115 fold higher affinity for ISG15-conjugated rather than Ub-modified substrates (18, 30). However,
116 it is unknown whether targeting PLP2 activity in an *in vitro* cell culture system or *in vivo* will
117 inhibit coronavirus replication. Furthermore, questions remain as to whether ISGylation itself is
118 antiviral against coronavirus infection and/or whether the PLP2 machinery *in vitro* targets ISGy-
119 lation directly to evade the host response.

120 In the present study, we infected USP18$^{-/-}$ mice with the coronavirus MHV-3 to evaluate
121 the involvement of the ISG15/USP18 pathway to the virulence of MHV-3-induced hepatitis. We
122 found that USP18$^{-/-}$ mice are more resistant to MHV-3 infection, but that the virus gradually
123 overcomes this protective effect. IFN type 1 and type 2 expression levels were not increased in
124 USP18$^{-/-}$ mice following infection by MHV-3, allowing us to study the role of increased baseline
125 ISGylation in the absence of IFN signalling. Silencing ISGylation reverses the antiviral milieu

126 and leads to increased MHV-3 replication. Both *in vitro* and *in vivo*, viral persistence is accom-
127 panied by increased expression of the PLP2 protein. PLP2 expression is important for allowing
128 viral replication; specific PLP inhibitors decreased viral protein expression. Overall, these results
129 demonstrate both the role and the limits of the antiviral effect of ISGylation in severe coronavi-
130 rus infection.
131

132 **Materials and Methods:**

133 **Animals**

134 C57BL/6 USP18$^{+/+}$ and USP18$^{-/-}$ mice between 6 -8 weeks old were used for experiments. These
135 mice were the kind gift of Dong Er Zhang (Scripps/UCSD). Animals were housed in SPF condi-
136 tions at the MaRS-TMDT Animal Resource Centre (Toronto) and were given chow and water *ad*
137 *libitum*. Following MHV-3 infection animals were housed in sterile cages in a level 2 facility in
138 the MBRC (Toronto). Mice infected with MHV-3 were sacrificed at humane endpoints. Animals
139 were treated according to the guidelines of the Canadian Council on Animal Care and were ap-
140 proved by the University Health Network Animal Care Committee.

141

142 **Isolation of Peritoneal exudative macrophages (PEM) and Hepatocytes**

143 The isolation of PEM has been previously described (28). Briefly, mice were injected with 2ml
144 of sterile 3% thioglycollate. Animals were sacrificed after 3 days and PEM were retrieved by
145 washing the intraperitoneal cavity with 10ml ice cold Hank's buffered salt solution (HBSS) (Life
146 Technologies). Cells were washed 2-fold, spun down at 300 × g and re-suspended in Dulbecco's
147 Modified Eagle Medium (DMEM) (Life Technologies) supplemented with L-Gln. Using this
148 method, the purity of PEM was found to be > 90% with a viability of >97% by Trypan blue ex-
149 clusion. For experiments, PEM were plated on polystyrene plates at a density of 1×10^6 cells/ml
150 and incubated for 24h at 37°C and 5% CO_2. Non-adherent cells were then washed away.
151 Primary hepatocytes were isolated as previously described (31, 32). Briefly, mice were anesthe-
152 tised with 50 mg/kg of pentobarbital i.p.. The portal vein was canulated with a 21-gauge needle.
153 The liver was flushed via the portal vena cava with perfusion solution (2.5mM EGTA in HBSS
154 without Ca^{2+} or Mg^{2+}) at 37°C and a rate of 7ml/min using an infusion pump for 3min. The liver

155 was then perfused with solution #2 (0.02% collagenase IV (Sigma-Aldrich) with calcium and
156 magnesium in HBSS) at the same pressure. The liver was then carefully harvested into a Petri
157 dish containing DMEM-15 and 1×10^{-7}M insulin (Sigma-Aldrich) and minced. This solution
158 was filtered through a 120 µm nylon mesh and centrifuged for 2min at 40 × g at room tempera-
159 ture (RT). Cells were washed 2 times with DMEM + insulin. Cells were counted on a hemocy-
160 tometer and viability was determined by Trypan blue exclusion. Hepatocytes were plated at a
161 density of 1×10^5 cells/ml in DMEM supplemented with 1×10^{-7}M insulin on a 6-well plate
162 (Corning Inc.). Hepatocytes were incubated for 2 hours and the medium was replaced with serum
163 free DMEM supplemented with 1×10^{-7}M insulin. Hepatocytes were inoculated with MHV-3
164 (multiplicity of infection (MOI) = 1, 0.1 or 0.01) and incubated for 1h. Cells were then washed
165 with serum free medium + 1×10^{-7}M insulin and cultured for the indicated time.
166

167 **Virus, viral infection and viral titering**

168 MHV-3 virus was grown to titers of 10-50 × 10^6 PFU/ml RPMI on confluent 17CL cells. To de-
169 termine viral titers, harvested cells or liver tissue, were lysed or homogenized in ice-cold
170 DMEM-10 using a TissueLyser (QIAGEN). MHV-3 titers were assessed on monolayers of L2
171 cells in a standard plaque assay (6). For *in vivo* studies mice were infected i.p. with 50 PFU of
172 MHV-3 and housed in sterile conditions. Animals were monitored daily and sacrificed at a hu-
173 mane end point.
174

175 **Histology**

176 Tissues were harvested and preserved in 10% buffered formalin. Fixed tissues were paraffin em-
177 bedded and cut into 5µm sections by the Department of Pathology at the Hospital for Sick Chil-

178 dren (Toronto). Sections were stained with Hematoxylin and Eosin using standard protocols (33).
179 Sections were scored in a blinded fashion by an experienced liver pathologist (M.J.P.). Sections
180 were assessed for inflammation, parenchymal changes and tissue necrosis.
181
182 **Measurement of alanine transaminase (ALT) and (aspartate aminotransferase)AST in the**
183 **serum**
184 Blood was harvested by cardiac puncture and was incubated for 10min at RT. Samples were
185 spun down at 2,000 × g and the serum was collected for analysis. ALT/AST levels were meas-
186 ured using the Vitro DT60 II Chemistry System (Ortho Clinical Diagnostics, Neckargemund,
187 Germany).
188
189 **Serum protein levels of type I and type II IFN**
190 Blood was harvested from mice by cardiac puncture. Serum was incubated at 4°C overnight
191 (O/N). The samples were centrifuged at 2,000 × g for 10min and the serum was removed to a
192 fresh tube. ELISA kits for IFN-α and IFN-β were purchased from PBL Interferon Source (Pis-
193 cataway Township, NJ, USA). The ELISA kit for IFN-γ was purchased from BioLegend Inc
194 (San Diego, CA, USA). ELISA tests were performed according to manufacturer's instructions.
195
196 **Real Time PCR**
197 Mice were infected with MHV-3 and sacrificed on the indicated day(s). Total RNA was ex-
198 tracted from liver tissue using TRIzol reagent (Invitrogen) according to manufacturer's specifica-
199 tions. The isolated RNA was treated with DNase (Qiagen) and the quality of the RNA was as-
200 sessed by measuring 260/280 on a Nanodrop spectrophotometer. 1µg of RNA was reverse tran-

201 scribed using the First Strand cDNA Synthesis Kit (GE Health Care) using random hexamer oli-
202 gonucleotides. The reverse transcriptase reaction was run as per manufacturer's specifications.
203 Primers used for Real Time PCR reactions were based on published and primer bank sequences.
204 The following primer sequences were used: mouse IFN-α forward primer 5'-
205 CTTTGGATTCCCGCAGGA-3'; mouse IFN-α reverse primer 5'- TGTAG-
206 GACAGGGATGGCTTGA-3'; mouse IFN-β forward primer 5'-
207 TGAATGGAAAGATCAACCTCACCTA-3'; mouse IFN-β reverse primer 5'-
208 CTCTTCTGCATCTTCTCCGTCA-3'; mouse IFN-γ forward primer 5'-
209 CAGCAACAGCAAGGCGAAA-3'; mouse IFN-γ reverse primer 5'-
210 CTGGACCTGTGGGTTGTTGAC-3'; mouse hypoxanthine phosphoribosyltransferase (HPRT)
211 forward primer 5'-GTTGGATACAGGCCAGACTTTGTT G-3'; mouse HPRT reverse primer 5'-
212 GATTCAACTTGCGCTCATCTTAGGC-3'; mouse glyceraldehyde 3-phosphate dehydrogenase
213 (GAPDH) forward primer 5'-ACAACTTTGGCATTGTGGAA-3'; mouse GAPDH reverse
214 primer 5'-GATGCAGGGATGATGTTCTG-3'; MHV-3 PLP2 forward primer 5'-
215 AAATGTGGCTTGTTTGATGC-3'; and, MHV-3 PLP2 reverse primer 5'-
216 CCTTCGCTAAGACCAAGGAC-3'.
217 Real Time PCR was performed on an ABI PRISM 7900H (Applied Biosystems) with SYBR
218 Green real time PCR master mix (Applied Biosystems) according to manufacturer's specifica-
219 tions using the 96-well plate format. Data was analyzed using SDS 2.2 Software (Applied Bio-
220 systems) using the standard curve method. Samples were normalized to HPRT and GAPDH.
221
222 **Western Blot (WB)**

223 Harvested tissues were homogenized and lysed in ice-cold cell lysis buffer. Cells from *in vitro*
224 cultures were lysed with 2 × Laemmli buffer and 0.1mM DTT. Protein concentrations were de-
225 termined by the Bradford assay. 20µg of proteins was visualized by 10% SDS-PAGE gel and
226 transferred to a nitrocellulose membrane (Pall). Membranes were probed with the following an-
227 tibodies: anti-nucleocapsid (N) protein mouse monoclonal (made in-house), anti-mouse β-actin
228 mouse monoclonal antibody (Sigma), anti-mouse ISG15 rabbit polyclonal antibody, anti-mouse
229 Ube1L goat polyclonal IgG, or anti-mouse STAT1 (p84/p91) rabbit polyclonal (Santa Cruz Bio-
230 technology). The corresponding horseradish peroxidase (HRP) conjugated secondary antibodies
231 were used: Sheep anti-mouse IgG (GE Healthcare), donkey anti-rabbit IgG (Santa Cruz Biotech-
232 nology) or a donkey anti goat IgG (Santa Cruz Biotechnology). Blots were developed using the
233 ECL system (Amersham Pharmacia Biotech).
234
235 **Silencing Ube1L expression**
236 Isolated primary hepatocytes were plated at a density of 1×10^5 cells/ml in DMEM. Cells were
237 incubated O/N at 37°C, 0.5% CO_2 whereupon cells reached 60-80% confluency. Cells were
238 transfected with Ube1L siRNA (Santa Cruz Biotechnology) as per manufacturer's instructions.
239 Briefly, cells were washed with transfection medium and then overlaid with transfection reagent
240 solution and incubated for 6 h at 37°C. DMEM medium including 10% FBS was added and the
241 cells were incubated a total of 24h. The medium was replaced with normal growth medium and
242 cells were infected with MHV-3 (MOI=1) ± IFN-α (PBL Interferon Source). Samples were har-
243 vested 12h p.i. using 200µl protein lysis buffer (BD bioscience), run on a 10% SDS PAGE gel
244 and visualized by WB.
245

246 **PLP2 Inhibition**

247 PLP2 inhibitors were generated in house according to Ratia *et al* (34). Isolated PEM were incu-
248 bated in the presence of MHV-3 (MOI=1) for 1h. Medium was washed away and fresh medium
249 ± 100µM inhibitor 6, 100µM inhibitor 7, 100µM GRL0617 or 100IU/ml IFN-α was added (PBL
250 Interferon Source). Cells were harvested at 9h p.i., run on a 10% SDS PAGE gel and visualized
251 by WB.

252

253 **Statistics**

254 Statistical analysis was performed using PRISM software version 5 (GraphPad Software Inc).
255 Survival curves were calculated using the Log-rank (Mantel-Cox) test.
256 Data analysis was performed using a 2-way ANOVA followed by a Bonferroni post-hoc test
257 unless otherwise noted. Data is represented as either mean ± SD or mean ± SEM as indicated.
258 Results with a p value below 0.05 were considered significant.

259

260

261

262

263

264 **Results**

265 **USP18$^{-/-}$ mice have increased survival following MHV-3 infection**

266 To test our hypothesis that ISGylation has an antiviral effect on murine hepatitis virus
267 (MHV)-3 infection we infected USP18$^{-/-}$ mice, which have high baseline levels of ISGylation,
268 and control USP18$^{+/+}$ mice with 50 pfu. MHV-3 (20). The infection of susceptible C57BL/6 mice
269 with MHV-3 induces a fulminant hepatitis with hepatocellular necrosis, sinusoid thrombosis,
270 strong cytokine induction and leads to death within 3-4 days p.i. (6). USP18$^{+/+}$ (C57BL/6) mice
271 survived a median of 4 days and observed the rapid development of symptoms characteristic of
272 MHV-3 infection (Figure 1A). By contrast, USP18$^{-/-}$ mice (C57BL/6) survived up to 10 days p.i.,
273 with a median survival of 8 days. The lengthened survival was accompanied by improved liver
274 histology at all time points. On day 3, all USP18$^{+/+}$ liver histology showed 40 to 50% focal ne-
275 crosis, and by day 4, 70-90% of the liver showed evidence of confluent necrosis (Figure 1B). In
276 comparison, USP18$^{-/-}$ livers on day 4 showed only small areas of focal necrosis affecting 5-10%
277 of the liver. MHV-3 infection of USP18$^{-/-}$ mice did gradually lead to widespread liver damage
278 (40-50% focal necrosis), though never as pronounced as in USP18$^{+/+}$ mice. Improved liver his-
279 tology in USP18$^{-/-}$ mice coincided with a decrease in the levels of serum transaminases (markers
280 of liver injury) and decreased viral titers compared to USP18$^{+/+}$ mice (Figure 1C-E). Histology,
281 viral titers and liver function in USP18$^{-/-}$ was improved at all time points compared with
282 USP18$^{+/+}$ mice. However, at day 7 p.i., the USP18$^{-/-}$ pathogenesis approached levels comparable
283 to USP18$^{+/+}$ mice at day 3 p.i. in all 3 of the measured criteria including histology, serum
284 transaminase levels and viral titers (Figure 1E). Therefore, the absence of USP18 confers an
285 early antiviral advantage against MHV-3 infection. However, USP18$^{-/-}$ mice ultimately suc-
286 cumbed to infection.

287

288 **MHV-3 infection does not induce type I IFN in USP18$^{-/-}$ mice**

289 USP18$^{-/-}$ mice have increased baseline cellular ISGylation levels and they have increased
290 sensitivity to Type I IFN signalling (20). Either of the two aspects of the USP18$^{-/-}$ phenotype
291 may explain the suppression of viral replication and decreased inflammatory response seen in
292 response to MHV-3 infection. In order to determine whether increased sensitivity to type 1 IFN
293 contributed to the suppression of MHV-3 replication in USP18$^{-/-}$ mice, we measured Type I IFN
294 (IFNα, IFNβ) induction by MHV-3 infection. In parallel we measured Type II IFN (IFNγ), as a
295 control pro-inflammatory cytokine. MHV-3 infection of USP18$^{+/+}$ mice induced strong mRNA
296 and protein expression of IFNα, IFNβ, and IFNγ in the liver and serum respectively. In USP18$^{-/-}$
297 mice, there was no induction of IFNα, IFNβ, or IFNγ hepatic mRNA and protein levels in re-
298 sponse to MHV-3 infection at all time points studied (Figure 2A-D). Similarly, MHV-3 infection
299 did not induce type I or type II IFN induction in USP18$^{-/-}$ primary hepatocytes (*data not shown*).
300 Finally, USP18$^{-/-}$ peritoneal exudative macrophages (PEM) that were infected with MHV-3 did
301 not show increased Type I IFN signalling, as seen by the absence of STAT1 phosphorylation
302 (*data not shown*). These data imply that the increased antiviral activity against MHV-3 observed
303 in the USP18$^{-/-}$ mice is not due to increased IFN production or signalling.

304

305 **Cellular ISGylation inhibits MHV-3 Replication**

306 Since the decrease in MHV-3 replication and mortality following infection of USP18$^{-/-}$
307 mice is not due to increased IFN or Type I IFN signalling, we asked whether decreased MHV-3
308 replication and mortality was due to increased levels of ISGylation (21). First, we examined
309 whether the decreased proliferation of MHV-3 in USP18$^{-/-}$ *in vivo* could be replicated *in vitro* in

310 primary hepatocytes. Hepatocytes isolated from USP18$^{+/+}$ and USP18$^{-/-}$ mice were infected with
311 MHV-3 (multiplicity of infection (MOI)=1) and viral titers were measured up to 48h p.i. (Figure
312 3A). USP18$^{+/+}$ hepatocytes reached peak MHV-3 titers, $2.09 \times 10^7 \pm 1.29 \times 10^6$ PFU, between
313 12-18h p.i. Viral titers remained elevated until 36h p.i, after which the levels started to decrease,
314 presumably due to cell death. Viral titers increased in USP18$^{-/-}$ hepatocytes with slower kinetics
315 than USP18$^{+/+}$ mice, with nearly a log decrease in MHV-3 titers at almost all time points. How-
316 ever, USP18$^{-/-}$ mice reached peak viral titers at 36h at $1.03 \times 10^7 \pm 2.31 \times 10^5$ PFU, more than
317 18h after USP18$^{+/+}$ peak titers. These *in vitro* results support the *in vivo* finding that MHV-3 viral
318 titers are suppressed in the presence of increased ISGylation. Although the viral titers in USP18$^{-/-}$
319 hepatocytes are suppressed initially, the virus eventually overwhelms the antiviral response. This
320 is similar to the extended survival seen in USP18$^{-/-}$ mice, but these mice ultimately succumb to
321 MHV-3 infection. Of note, at early time points following MHV-3 inoculation, namely 1h, 3h and
322 6h, viral titers of USP18$^{+/+}$ and USP18$^{-/-}$ mice do not differ significantly (2-way ANOVA with
323 Bonferroni post-hoc test). This suggests that viral binding and entry into the cell may not be af-
324 fected by interferon stimulated gene (ISG)-15 antiviral activity however, further studies are re-
325 quired to differentiate the effects of ISGylation on viral binding and entry and viral replication.
326 The amount of ISG15-conjugated proteins is markedly higher in USP18$^{-/-}$ hepatocytes
327 than USP18$^{+/+}$ hepatocytes at all time points following MHV-3 infection (Figure 3B). The ex-
328 pression of viral nucleocapsid (N) protein is detectable by WB starting at 6h p.i. in USP18$^{+/+}$
329 hepatocytes and continues to accumulate until 18h (Figure 3B) when peak N protein expression
330 coincides with peak viral titers (Figure 3A). By contrast, in USP18$^{-/-}$ hepatocytes, overall N pro-
331 tein accumulation is decreased and is delayed compared to USP18$^{+/+}$ hepatocytes. These *in vitro*

332 data mirror the *in vivo* results, and suggest that high ISGylation levels are an intrinsic antiviral
333 force against coronavirus in USP18$^{-/-}$ mice.
334
335 To determine whether ISGylation is causally linked to MHV-3 virus production we
336 knocked down the ISG15 pathway E1 enzyme Ube1L to block ISGylation. Ube1L is the unique
337 activating enzyme of the ISG15/USP18 pathway, and forms an ATP-dependent thioester bond
338 with ISG15 (11, 35). Ube1L knockdown in primary USP18$^{+/+}$ murine hepatocytes decreased
339 Ube1L protein and attenuated the increase in ISGylation that follows exposure of cells to IFN-α
340 (Figure 4). Ube1L silencing in USP18$^{+/+}$ primary cells infected with MHV-3 abrogates ISGylation
341 and leads to increased N protein expression. As shown previously (Figure 3B), N protein levels
342 are markedly decreased in USP18$^{-/-}$ compared to USP18$^{+/+}$ cells at 12h p.i.. The effect of Ube1L
343 knockdown is more prominent in USP18$^{-/-}$ primary cells Ube1L silencing markedly decreased
344 protein ISGylation in USP18$^{-/-}$ primary cells from high baseline levels of ISGylation, although
345 ISGylation levels remained at elevated levels following MHV-3 infection compared to control
346 hepatocytes. Following both MHV-3 infection and Ube1L knock down, the levels of ISGylated
347 proteins drops further compared to Ube1L knock down alone (Figure 4) and, N protein expres-
348 sion, the surrogate of MHV-3 replication, reached levels of expression higher than induced by
349 MHV-3 infection alone. MHV-3 infection decreased ISGylation in both USP18$^{+/+}$ and USP18$^{-/-}$
350 mice. The former however was only observed following treatment with IFN-α which strongly
351 induces ISGylation. In the absence of IFN-α, no ISGylation is detected by WB. These data sug-
352 gest that the Ube1L conjugation of ISG15 to target proteins, and the subsequent accumulation of
353 ISGylated proteins mediates an antiviral effect against MHV-3.
354

355 **The effect of PLP inhibitors on MHV-3 infection**

356 Since there is an observed decrease in ISGylation in USP18$^{-/-}$ following MHV-3 infection, we
357 next asked whether the MHV-3 PLP2 protein is the mechanism through which MHV-3 ulti-
358 mately escapes the effect of host ISGylation. To this end, we treated MHV-3 infected cells with
359 synthetic PLP inhibitors. The PLP inhibitors are non-covalent cysteine inhibitor compounds gen-
360 erated against the catalytic residues of the SARS Coronavirus PLpro (34). PLP inhibitors in-
361 creased ISGylation levels in USP18$^{+/+}$ PEM. No observable change in ISGylation was observed
362 in USP18$^{-/-}$ PEM even in less saturated blots (*data not shown*) due perhaps to already high base-
363 line levels of ISGylation in USP18$^{-/-}$ PEM. USP18$^{+/+}$ PEM infected with MHV-3 showed strong
364 expression of N protein at 9h p.i. Treatment of USP18$^{+/+}$ PEM with PLpro inhibitors resulted in
365 decreased levels of N protein production (Figure 5). Treatment with GRL0617, the PLP inhibitor
366 with the highest binding capacity (34), resulted in the greatest decrease in viral N protein produc-
367 tion. In MHV-3 infected USP18$^{-/-}$ PEM, where baseline levels of ISGylated proteins are high
368 (21), the expression of N protein is significantly decreased compared to wildtype PEM. The ex-
369 pression of N protein is even more inhibited following treatment with all PLpro inhibitors. By
370 WB analysis, GRL0617 completely inhibited the expression of N protein. Consistent with these
371 data, viral titers were decreased in the presence of PLP2 inhibitors in both USP18$^{+/+}$ and USP18^{-}
372 $^{/-}$ PEM (*data not shown*). Similar data was obtained for hepatocytes (data not shown). Overall
373 these results suggest that MHV-3 proliferation and evasion from the cellular antiviral ISGylation
374 milieu is dependent on PLP2 activity.

375

376 **ISGylation delays onset of MHV-3 production and death *in vivo***

377 Above, we showed that ISGylation *in vitro* exerts an antiviral pressure on MHV-3 coro-
378 navirus replication. However, this antiviral pressure is overcome as the virus replicates and ex-
379 presses the deubiquitinase protein (DUB) PLP2. In order to test whether this holds true *in vivo*,
380 we inoculated USP18$^{+/+}$ and USP18$^{-/-}$ animals with 50 PFU of MHV-3 i.p. and measured ISGyla-
381 tion and PLP2 levels in whole liver tissue. As before, USP18$^{+/+}$ mice became moribund and were
382 euthanized by day 4 p.i. Liver protein ISGylation increased and peaked at day 3p.i. (Figure 6); N
383 protein was first detectable at day 2 and increased steadily until the animals were euthanized on
384 day 4. By contrast, USP18$^{-/-}$ mice have higher baseline liver ISGylation levels throughout the
385 entire course of infection, and MHV-3 replication as seen by N protein expression was first de-
386 tected at day 6 p.i.. Concurrently, we measured viral expression of *plp2* mRNA. *Plp2* mRNA ex-
387 pression increased as N protein expression increased and *plp2* expression was delayed in USP18^{-}
388 $^{/-}$ mice compared to control mice (Figure 7). These data are consistent with the ability of in-
389 creased PLP2 to gradually overwhelm the antiviral effect of ISGylation *in vivo* by stripping
390 ISG15 from target proteins.
391
392

393 **Discussion**

394 During the innate immune response, ISGylation is an important barrier against viral in-
395 fection. ISG are up-regulated following the activation of type I IFN signalling and have various
396 functions in the innate immune response including the feed-back regulation of the host immune
397 response and antiviral activities (36-41). ISG15 is one of the most abundantly up-regulated ISG.
398 In this study we show that ISG15 conjugation (ISGylation) has antiviral activity in a model of
399 severe coronavirus infection and that this antiviral activity is independent of type I IFN signal-
400 ling.

401 Studies have shown that ISGylation is antiviral against several viruses including, influ-
402 enza B virus, sindbis virus, sendai virus and vaccinia virus (15, 41-44). ISG15 and IFNαβ recep-
403 tor double deficient mice, which lack ISG15 and have an impaired ability to induce ISG follow-
404 ing IFNα/β stimulation, were rescued against Sindbis virus induced lethality by expressing
405 ISG15 (42, 43). The antiviral activity associated with ISG15 is dependent on the conjugation of
406 ISG15 to target proteins, as the mutation of the ISG15 C-terminal isopeptidase target motif ren-
407 dered ISGylation ineffective against Sindbis Virus (42). However, ISGylation is permissive for
408 certain viruses. We and others have demonstrated that cellular ISGylation is necessary for the
409 efficient replication of Hepatitis C Virus (25, 45). Our data demonstrate that ISGylation is antivi-
410 ral to MHV-3 infection. In USP18$^{-/-}$ mice, where ISGylation levels are high, there was a signifi-
411 cant decrease in viral N protein expression *in vitro* and *in vivo* that coincided with prolonged
412 survival. We attribute the prolongation in survival to the antiviral effect of ISGylation, since we
413 did not observe the induction of a type I or type II IFN response in the USP18$^{-/-}$ animals. The
414 role of ISGylation was confirmed by Ube1L knockdown experiments, in which silencing Ube1L
415 in primary hepatocytes reversed the antiviral activity of ISGylation. (Figure 4). These data are in

416 accordance with studies in which both Ube1L$^{-/-}$ mice, which lack the ability to conjugate ISG15
417 to target proteins, and ISG15$^{-/-}$ mice were more sensitive to Sindbis Virus infection (43, 46) than
418 wildtype animals. Therefore, our data provides another example of the antiviral nature of ISGy-
419 lation activity but in a novel context, coronavirus infection.

420 Coronaviruses evade the host innate immune response by interfering with the induction
421 of IFN (47-52). MHV-3 infection of USP18$^{+/+}$ mice resulted in markedly increased Type I IFN
422 mRNA and protein (Fig 2A-D). By contrast, MHV-3 infection of USP18$^{-/-}$ mice resulted in little,
423 if any, IFN production at either the mRNA or protein levels. At first glance this is surprising,
424 since USP18$^{-/-}$ mice are hypersensitive to IFN, and we expected that any IFN-β produced upon
425 exposure to MHV-3 virus would stimulate IFN-α production in a positive feedback loop (53).
426 Furthermore, the increased ISGylation observed in USP18$^{-/-}$ cells would be expected to lead to
427 increased IFN production since the direct ISGylation of interferon regulatory transcription fac-
428 tor-3 (IRF-3) prolongs the activation of IRF-3 and results in increased expression of IFN-β and
429 other ISGs (41). However, we observed an almost complete absence of type I IFN production in
430 response to MHV-3. While it is tempting to ascribe the lack of IFN production to the increased
431 ISGylation seen in USP18$^{-/-}$ cells, this is unlikely. Firstly, USP18 was shown to regulate type I
432 IFN induction independent of isopeptidase activity and that ISG15 antiviral activity is independ-
433 ent of IFN signalling (22, 43). Secondly, the observed lack of a type I IFN response may also be
434 due to differences in the immune cell phenotype of USP18$^{-/-}$ mice. Cong *et al* described a
435 USP18-dependent but ISGylation-independent difference in dendritic cell maturation (54). Simi-
436 larly, we have observed a fundamental difference in the phenotype of USP18$^{-/-}$ macrophages and
437 kupffer cells, with a shift from the M1 pro-inflammatory phenotype in USP18$^{+/+}$ mice to an M2
438 regulatory phenotype in USP18$^{-/-}$ mice (*manuscript in preparation*). This result may suggest that

439 the fact that MHV-3 does not induce IFN is not specific to the virus but the phenotype of the
440 USP18$^{-/-}$ macrophages and dendritic cells, both of which are key producers of hepatic IFN (23,
441 53, 55). Differences in immune cell phenotype and the consequent lack of IFN production in
442 USP18$^{-/-}$ mice raise the possibility of confounding immune effects in our *in vivo* data. However,
443 the lack of a type I IFN response in the USP18$^{-/-}$ mice would be expected to promote viral repli-
444 cation, but we observed the reverse effect. The lack of IFN signalling thus allows us to attribute
445 our results to ISGylation as opposed to IFN signalling in USP18$^{-/-}$ mice.

446 The mechanism by which ISGylation exerts an antiviral activity against MHV-3 is un-
447 clear. ISGylation can modulate viral production in one of two ways: by being conjugated to viral
448 proteins in a manner that disrupts the viral life cycle, or by conjugating to host proteins that play
449 a role in the viral life cycle or in the host innate immune response (11). In the context of the IS-
450 Gylation of viral proteins, the conjugation of ISG15 to the Influenza A NS1 viral protein is anti-
451 viral to influenza A infection in humans (39). ISGylation of NS1 prevents its association with
452 importin-α and its subsequent translocation to the nucleus, ultimately inhibiting viral replication
453 (38). In an example of host protein modification, the ISGylation of host 4E homologous protein
454 (4EHP) protein exerts an antiviral effect by interfering with viral (and host) protein translation.
455 4EHP is a 5′ mRNA cap binding protein that competes with eukaryotic initiation factors-4 (eIF4)
456 to suppress translation. The ISGylation of 4EHP increases its RNA binding capacity, and
457 strongly suppresses translation of both host and viral proteins during the innate immune response
458 (37). Lastly, another group reported a mechanism that incorporates both host and viral protein
459 ISGylation: the antiviral pressure of ISGylation observed in this model is exerted by the indis-
460 criminate ISGylation of newly synthesized proteins that follows IFN stimulation or USP18 dele-
461 tion (36). The nonspecific ISGylation of the nascent subset of each protein population present in

462 the cell has been suggested to disrupt viral proliferation through a dominant negative effect. Such
463 an effect has been shown in models of human papilloma virus (HPV) and HIV infection (36, 56)
464 and is consistent with our finding that the effect of ISGylation blunts viral replication but does
465 not abrogate it altogether. Further studies are necessary to determine the mechanism by which
466 ISGylation specifically delays MHV-3 replication.

467 Although ISGylation exerts an antiviral pressure on the MHV-3 coronavirus, the virus
468 ultimately overcomes this pressure both *in vitro* and *in vivo*. Viral titers in states of increased
469 ISGylation (USP18$^{-/-}$), approach peak levels seen in states of low ISGylation (USP18$^{+/+}$) follow-
470 ing a 3-day delay. Additionally, N protein production and PLP2 expression levels increase while
471 ISGylation levels in USP18$^{-/-}$ mice decrease (Figure 6-7). All Coronaviruses express a DUB that
472 removes both ubiquitin and ISG15 from conjugated proteins (29, 57, 58). PLPs are multifunc-
473 tional viral proteins and have several functions relevant to coronavirus production within the host
474 cell including the processing of the viral polyprotein. In our study, some of the inhibitory effect
475 on MHV-3 production that follows treatment with PLpro inhibitors may be due to this effect (34,
476 51). However, treatment of wildtype PEM and hepatocytes with PLpro inhibitors increased cellu-
477 lar ISGylation following infection, and inhibited viral N protein expression (Fig 5). Our data
478 therefore, may be the result of both nsp3 cleavage and ISGylation but, it definitely contributes to
479 the stripping of ISG15 from target proteins. Regardless of the relative contributions of each
480 mode of action, these data support the use of PLP2 inhibitors as one arm of treatment against
481 coronavirus infection. The DUB activity may thus contribute to the evasion of the host antiviral
482 response by altering immune responses through deISGylation or by reactivating ISGylated viral
483 proteins.

484 We have previously shown that increasing ubiquitination exerts an antiviral effect on
485 coronavirus replication (28), and in this study we have shown that ISGylation exerts a similar
486 effect. Both DUB functions of PLP2 would favour MHV3 replication, though the PLP2 has more
487 affinity for ISGylated proteins than for ubiquitinated proteins and therefore may be more rele-
488 vant as an antiviral mechanism (29, 30, 59).

489 Overall our data are consistent with the ability of ISGylation to exert an antiviral pressure
490 in a model of severe MHV3 coronavirus infection. This effect is most marked in the setting of
491 USP18 deletion, suggesting that targeting USP18 might have a clinical benefit in treating severe
492 Coronavirus infections. However, our data also strongly argue that treatment of a Coronavirus
493 infection should be multi-faceted, since the virus has evolved mechanisms to overwhelm the an-
494 tiviral effect of ISGylation – one of the chief effector mechanisms of IFN. As illustrated by this
495 study, coronavirus can escape the host antiviral response in a number of ways that are independ-
496 ent of IFN signalling. IFN therapy, the current treatment for Coronavirus infection, should be
497 considered in conjunction with other therapies, such as the inhibition of PLP activity and protea-
498 some inhibition to comprehensively counter the effects of the viral DUB (28).

499

500 **Acknowledgements**

501 Special thanks to Dong Er Zhang for the gift of the USP18$^{-/-}$ mice.
502 This research was supported by the Canadian Institute of Health Research (grant # 200622).

503

504

505

506 **References**

507

508 1. Rota PA, Oberste MS, Monroe SS, Nix WA, Campagnoli R, Icenogle JP, Penaranda S,
509 Bankamp B, Maher K, Chen MH, Tong S, Tamin A, Lowe L, Frace M, DeRisi JL, Chen
510 Q, Wang D, Erdman DD, Peret TC, Burns C, Ksiazek TG, Rollin PE, Sanchez A, Liffick
511 S, Holloway B, Limor J, McCaustland K, Olsen-Rasmussen M, Fouchier R, Gunther S,
512 Osterhaus AD, Drosten C, Pallansch MA, Anderson LJ, Bellini WJ. 2003.
513 Characterization of a novel coronavirus associated with severe acute respiratory
514 syndrome. Science 300:1394-1399.

515 2. WHO 15 Aug 2003, posting date. Summary table of SARS cases by country, 1
516 November 2002 - 7 August 2003 Global Alert and Response (GAR). [Online.]

517 3. WHO 16 Feb 2013, posting date. Novel coronavirus infection – update Global Alert and
518 Response (GAR). [Online.]

519 4. Perlman S, Dandekar AA. 2005. Immunopathogenesis of coronavirus infections:
520 implications for SARS. Nat Rev Immunol 5:917-927.

521 5. Bergmann CC, Lane TE, Stohlman SA. 2006. Coronavirus infection of the central
522 nervous system: host-virus stand-off. Nat Rev Microbiol 4:121-132.

523 6. Levy GA, Leibowitz JL, Edgington TS. 1981. Induction of monocyte procoagulant
524 activity by murine hepatitis virus type 3 parallels disease susceptibility in mice. J Exp
525 Med 154:1150-1163.

526 7. Marsden PA, Ning Q, Fung LS, Luo X, Chen Y, Mendicino M, Ghanekar A, Scott JA,
527 Miller T, Chan CWY, Chan MWC, He W, Gorczynski RM, Grant DR, Clark DA,
528 Phillips MJ, Levy GA. 2003. The Fgl2/fibroleukin prothrombinase contributes to
529 immunologically mediated thrombosis in experimental and human viral hepatitis. Journal
530 of Clinical Investigation 112:58-66.

531 8. Pope M, Rotstein O, Cole E, Sinclair S, Parr R, Cruz B, Fingerote R, Chung S,
532 Gorczynski R, Fung L, et al. 1995. Pattern of disease after murine hepatitis virus strain 3
533 infection correlates with macrophage activation and not viral replication. Journal of
534 virology 69:5252-5260.

535 9. McGilvray ID, Lu Z, Wei AC, Dackiw AP, Marshall JC, Kapus A, Levy G, Rotstein OD.
536 1998. Murine hepatitis virus strain 3 induces the macrophage prothrombinase fgl-2
537 through p38 mitogen-activated protein kinase activation. The Journal of biological
538 chemistry 273:32222-32229.

539 10. Farrell PJ, Broeze RJ, Lengyel P. 1979. Accumulation of an mRNA and protein in
540 interferon-treated Ehrlich ascites tumour cells. Nature 279:523-525.

541 11. Lenschow DJ. 2010. Antiviral Properties of ISG15. Viruses 2:2154-2168.

542 12. Giannakopoulos NV, Luo JK, Papov V, Zou W, Lenschow DJ, Jacobs BS, Borden EC, Li
543 J, Virgin HW, Zhang DE. 2005. Proteomic identification of proteins conjugated to ISG15
544 in mouse and human cells. Biochem Biophys Res Commun 336:496-506.

545 13. Zhao C, Denison C, Huibregtse JM, Gygi S, Krug RM. 2005. Human ISG15 conjugation
546 targets both IFN-induced and constitutively expressed proteins functioning in diverse
547 cellular pathways. Proc Natl Acad Sci U S A 102:10200-10205.

548 14. Malakhov MP. 2003. High-throughput Immunoblotting. UBIQUITIN-LIKE PROTEIN
549 ISG15 MODIFIES KEY REGULATORS OF SIGNAL TRANSDUCTION. Journal of
550 Biological Chemistry 278:16608-16613.

551 15. Osiak A, Utermohlen O, Niendorf S, Horak I, Knobeloch KP. 2005. ISG15, an
552 Interferon-Stimulated Ubiquitin-Like Protein, Is Not Essential for STAT1 Signaling and
553 Responses against Vesicular Stomatitis and Lymphocytic Choriomeningitis Virus.
554 Molecular and Cellular Biology 25:6338-6345.

555 16. Jeon YJ, Choi JS, Lee JY, Yu KR, Kim SM, Ka SH, Oh KH, Il Kim K, Zhang D-E, Bang
556 OS, Ha Chung C. 2009. ISG15 modification of filamin B negatively regulates the type I
557 interferon-induced JNK signalling pathway. EMBO reports 10:374-380.

558 17. Zou W, Papov V, Malakhova O, Kim KI, Dao C, Li J, Zhang D-E. 2005. ISG15
559 modification of ubiquitin E2 Ubc13 disrupts its ability to form thioester bond with
560 ubiquitin. Biochemical and Biophysical Research Communications 336:61-68.

561 18. Malakhov MP. 2002. UBP43 (USP18) Specifically Removes ISG15 from Conjugated
562 Proteins. Journal of Biological Chemistry 277:9976-9981.

563 19. Ritchie KJ. 2002. Dysregulation of protein modification by ISG15 results in brain cell
564 injury. Genes & Development 16:2207-2212.

565 20. Ritchie KJ, Hahn CS, Kim KI, Yan M, Rosario D, Li L, de la Torre JC, Zhang D-E.
566 2004. Role of ISG15 protease UBP43 (USP18) in innate immunity to viral infection.
567 Nature Medicine 10:1374-1378.

568 21. Malakhova OA. 2003. Protein ISGylation modulates the JAK-STAT signaling pathway.
569 Genes & Development 17:455-460.

570 22. Malakhova OA, Kim KI, Luo JK, Zou W, Kumar KG, Fuchs SY, Shuai K, Zhang DE.
571 2006. UBP43 is a novel regulator of interferon signaling independent of its ISG15
572 isopeptidase activity. EMBO J 25:2358-2367.

573 23. Woods MW, Kelly JN, Hattlmann CJ, Tong JG, Xu LS, Coleman MD, Quest GR, Smiley
574 JR, Barr SD. 2011. Human HERC5 restricts an early stage of HIV-1 assembly by a
575 mechanism correlating with the ISGylation of Gag. Retrovirology 8:95.

576 24. Chen L, Sun J, Meng L, Heathcote J, Edwards AM, McGilvray ID. 2010. ISG15, a
577 ubiquitin-like interferon-stimulated gene, promotes hepatitis C virus production in vitro:
578 implications for chronic infection and response to treatment. J Gen Virol 91:382-388.

579 25. Chen L, Borozan I, Sun J, Guindi M, Fischer S, Feld J, Anand N, Heathcote J, Edwards
580 AM, McGilvray ID. 2010. Cell-Type Specific Gene Expression Signature in Liver
581 Underlies Response to Interferon Therapy in Chronic Hepatitis C Infection.
582 Gastroenterology 138:1123-1133.e1123.

583 26. Chen L, Borozan I, Feld J, Sun J, Tannis L-L, Coltescu C, Heathcote J, Edwards AM,
584 McGilvray ID. 2005. Hepatic Gene Expression Discriminates Responders and

585 Nonresponders in Treatment of Chronic Hepatitis C Viral Infection. Gastroenterology
586 128:1437-1444.

587 27. McGilvray I, Feld JJ, Chen L, Pattullo V, Guindi M, Fischer S, Borozan I, Xie G, Selzner
588 N, Heathcote EJ, Siminovitch K. 2012. Hepatic cell-type specific gene expression better
589 predicts HCV treatment outcome than IL28B genotype. Gastroenterology 142:1122-1131
590 e1121.

591 28. Ma XZ, Bartczak A, Zhang J, Khattar R, Chen L, Liu MF, Edwards A, Levy G,
592 McGilvray ID. 2010. Proteasome inhibition in vivo promotes survival in a lethal murine
593 model of severe acute respiratory syndrome. Journal of virology 84:12419-12428.

594 29. Barretto N, Jukneliene D, Ratia K, Chen Z, Mesecar AD, Baker SC. 2005. The Papain-
595 Like Protease of Severe Acute Respiratory Syndrome Coronavirus Has Deubiquitinating
596 Activity. Journal of virology 79:15189-15198.

597 30. Lindner HA, Lytvyn V, Qi H, Lachance P, Ziomek E, Ménard R. 2007. Selectivity in
598 ISG15 and ubiquitin recognition by the SARS coronavirus papain-like protease. Archives
599 of Biochemistry and Biophysics 466:8-14.

600 31. Selzner N, Liu H, Boehnert MU, Adeyi OA, Shalev I, Bartczak AM, Xue-Zhong M,
601 Manuel J, Rotstein OD, McGilvray ID, Grant DR, Phillips MJ, Levy GA, Selzner M.
602 2012. FGL2/fibroleukin mediates hepatic reperfusion injury by induction of sinusoidal
603 endothelial cell and hepatocyte apoptosis in mice. J Hepatol 56:153-159.

604 32. McQueen CA, Williams GM. 1987. The hepatocyte primary culture/DNA repair test
605 using hepatocytes from several species. Cell Biol Toxicol 3:209-218.

606 33. De Albuquerque N, Baig E, Ma X, Zhang J, He W, Rowe A, Habal M, Liu M, Shalev I,
607 Downey GP, Gorczynski R, Butany J, Leibowitz J, Weiss SR, McGilvray ID, Phillips
608 MJ, Fish EN, Levy GA. 2006. Murine hepatitis virus strain 1 produces a clinically
609 relevant model of severe acute respiratory syndrome in A/J mice. Journal of virology
610 80:10382-10394.

611 34. Ratia K, Pegan S, Takayama J, Sleeman K, Coughlin M, Baliji S, Chaudhuri R, Fu W,
612 Prabhakar BS, Johnson ME, Baker SC, Ghosh AK, Mesecar AD. 2008. A noncovalent
613 class of papain-like protease/deubiquitinase inhibitors blocks SARS virus replication.
614 Proceedings of the National Academy of Sciences 105:16119-16124.

615 35. Yuan W, Krug RM. 2001. Influenza B virus NS1 protein inhibits conjugation of the
616 interferon (IFN)-induced ubiquitin-like ISG15 protein. EMBO J 20:362-371.

617 36. Durfee LA, Lyon N, Seo K, Huibregtse JM. 2010. The ISG15 Conjugation System
618 Broadly Targets Newly Synthesized Proteins: Implications for the Antiviral Function of
619 ISG15. Molecular Cell 38:722-732.

620 37. Okumura F, Zou W, Zhang DE. 2007. ISG15 modification of the eIF4E cognate 4EHP
621 enhances cap structure-binding activity of 4EHP. Genes Dev 21:255-260.

622 38. Zhao C, Hsiang TY, Kuo RL, Krug RM. 2010. ISG15 conjugation system targets the
623 viral NS1 protein in influenza A virus-infected cells. Proc Natl Acad Sci U S A
624 107:2253-2258.

625 39. Hsiang TY, Zhao C, Krug RM. 2009. Interferon-induced ISG15 conjugation inhibits
626 influenza A virus gene expression and replication in human cells. Journal of virology
627 83:5971-5977.

628 40. Liu SY, Sanchez DJ, Cheng G. 2011. New developments in the induction and antiviral
629 effectors of type I interferon. Curr Opin Immunol 23:57-64.

630 41. Shi HX, Yang K, Liu X, Liu XY, Wei B, Shan YF, Zhu LH, Wang C. 2010. Positive
631 Regulation of Interferon Regulatory Factor 3 Activation by Herc5 via ISG15
632 Modification. Molecular and Cellular Biology 30:2424-2436.

633 42. Lenschow DJ, Giannakopoulos NV, Gunn LJ, Johnston C, O'Guin AK, Schmidt RE,
634 Levine B, Virgin HWt. 2005. Identification of interferon-stimulated gene 15 as an
635 antiviral molecule during Sindbis virus infection in vivo. Journal of virology 79:13974-
636 13983.

637 43. Lenschow DJ, Lai C, Frias-Staheli N, Giannakopoulos NV, Lutz A, Wolff T, Osiak A,
638 Levine B, Schmidt RE, Garcia-Sastre A, Leib DA, Pekosz A, Knobeloch KP, Horak I,
639 Virgin HWt. 2007. IFN-stimulated gene 15 functions as a critical antiviral molecule
640 against influenza, herpes, and Sindbis viruses. Proc Natl Acad Sci U S A 104:1371-1376.

641 44. Guerra S, Caceres A, Knobeloch KP, Horak I, Esteban M. 2008. Vaccinia virus E3
642 protein prevents the antiviral action of ISG15. PLoS Pathog 4:e1000096.

643 45. Broering R, Zhang X, Kottilil S, Trippler M, Jiang M, Lu M, Gerken G, Schlaak JF.
644 2010. The interferon stimulated gene 15 functions as a proviral factor for the hepatitis C
645 virus and as a regulator of the IFN response. Gut 59:1111-1119.

646 46. Giannakopoulos NV, Arutyunova E, Lai C, Lenschow DJ, Haas AL, Virgin HW. 2009.
647 ISG15 Arg151 and the ISG15-Conjugating Enzyme UbE1L Are Important for Innate
648 Immune Control of Sindbis Virus. Journal of virology 83:1602-1610.

649 47. Zhou H, Perlman S. 2007. Mouse hepatitis virus does not induce Beta interferon
650 synthesis and does not inhibit its induction by double-stranded RNA. Journal of virology
651 81:568-574.

652 48. Versteeg GA, Bredenbeek PJ, van den Worm SH, Spaan WJ. 2007. Group 2
653 coronaviruses prevent immediate early interferon induction by protection of viral RNA
654 from host cell recognition. Virology 361:18-26.

655 49. Sun L, Xing Y, Chen X, Zheng Y, Yang Y, Nichols DB, Clementz MA, Banach BS, Li
656 K, Baker SC, Chen Z. 2012. Coronavirus Papain-like Proteases Negatively Regulate
657 Antiviral Innate Immune Response through Disruption of STING-Mediated Signaling.
658 PloS one 7:e30802.

659 50. Spiegel M, Pichlmair A, Martinez-Sobrido L, Cros J, Garcia-Sastre A, Haller O, Weber
660 F. 2005. Inhibition of Beta interferon induction by severe acute respiratory syndrome
661 coronavirus suggests a two-step model for activation of interferon regulatory factor 3.
662 Journal of virology 79:2079-2086.

663 51. Clementz MA, Chen Z, Banach BS, Wang Y, Sun L, Ratia K, Baez-Santos YM, Wang J,
664 Takayama J, Ghosh AK, Li K, Mesecar AD, Baker SC. 2010. Deubiquitinating and
665 Interferon Antagonism Activities of Coronavirus Papain-Like Proteases. Journal of
666 virology 84:4619-4629.

667 52. Devaraj SG, Wang N, Chen Z, Tseng M, Barretto N, Lin R, Peters CJ, Tseng CTK, Baker
668 SC, Li K. 2007. Regulation of IRF-3-dependent Innate Immunity by the Papain-like
669 Protease Domain of the Severe Acute Respiratory Syndrome Coronavirus. Journal of
670 Biological Chemistry 282:32208-32221.

671 53. Theofilopoulos AN, Baccala R, Beutler B, Kono DH. 2005. Type I interferons
672 (alpha/beta) in immunity and autoimmunity. Annu Rev Immunol 23:307-336.

673 54. Cong XL, Lo MC, Reuter BA, Yan M, Fan JB, Zhang DE. 2012. Usp18 Promotes
674 Conventional CD11b+ Dendritic Cell Development. The Journal of Immunology
675 188:4776-4781.

676 55. Rose KM, Weiss SR. 2009. Murine Coronavirus Cell Type Dependent Interaction with
677 the Type I Interferon Response. Viruses 1:689-712.

678 56. Lee SK, Harris J, Swanstrom R. 2009. A strongly transdominant mutation in the human
679 immunodeficiency virus type 1 gag gene defines an Achilles heel in the virus life cycle.
680 Journal of virology 83:8536-8543.

681 57. Lindner HA, Fotouhi-Ardakani N, Lytvyn V, Lachance P, Sulea T, Menard R. 2005. The
682 Papain-Like Protease from the Severe Acute Respiratory Syndrome Coronavirus Is a
683 Deubiquitinating Enzyme. Journal of virology 79:15199-15208.

684 58. Ratia K. 2006. Severe acute respiratory syndrome coronavirus papain-like protease:
685 Structure of a viral deubiquitinating enzyme. Proceedings of the National Academy of
686 Sciences 103:5717-5722.

687 59. Chen Z, Wang Y, Ratia K, Mesecar AD, Wilkinson KD, Baker SC. 2007. Proteolytic
688 Processing and Deubiquitinating Activity of Papain-Like Proteases of Human
689 Coronavirus NL63. Journal of virology 81:6007-6018.

690

691 **Figure Legends**

692 **Figure 1: USP18$^{-/-}$ mice showed delayed morbidity and death following MHV-3 infection**
693 A) Survival curve of USP18$^{+/+}$ and USP18$^{-/-}$ mice following infection with 50 pfu. MHV-3 i.p..
694 USP18$^{-/-}$ survival was prolonged up to 10 days with a median survival of 8 days compared to 4
695 days for control mice. n=10 per group. $p<0.0001$ using the Logrank test for trend. B) H&E stain-
696 ing of livers from USP18$^{+/+}$ and USP18$^{-/-}$ mice at days 0, 3, 4, and 7 p.i.. Black arrows point to
697 areas of focal necrosis. Photomicrographs at day 4 and day 7 for USP$^{+/+}$ and USP$^{-/-}$ mice respec-
698 tively show confluent necrosis of the liver. Magnification 40x. Photomicrographs are representa-
699 tive of each study group. C&D) The increase in liver markers of injury, AST and ALT, was de-
700 layed in USP18$^{-/-}$ mice. AST and ALT were measured and represented as log(U/L) ± SD. E)
701 USP18$^{-/-}$ mice show decreased viral titers. Viral titers were measured daily until day 4 and on
702 day 7 only in USP18$^{-/-}$ mice using a standard plaque assay. Data is represented as the mean
703 log(PFU/g) ± SD. *** $p<0.001$, ** $p<0.01$, *$p<0.05$.

704

705 **Figure 2: The IFN response to MHV-3 is blunted in USP18$^{-/-}$ mice**
706 Animals infected with MHV-3 were sacrificed on Day 0 through 4 with an additional measure-
707 ment at day 7 for USP18$^{-/-}$ mice (USP18$^{+/+}$ succumbed to disease by day 4 p.i.).
708 (A) mRNA expression of both type I and type II IFN is inhibited in USP18$^{-/-}$ mice. mRNA was
709 harvested from livers at USP18$^{+/+}$ or USP18$^{-/-}$ mice infected with 50 PFU. of MHV-3 and sacri-

710 ficed day 3 p.i.. (B-D) Serum levels of IFN were measured by ELISA. (B) IFN-α, (C) IFN-β and
711 (D) IFN-γ levels in the plasma were absent in the USP18$^{-/-}$ mice whereas USP18$^{+/+}$ were able to
712 induce type I and type II IFN responses. Data is represented as mean ± SD. (A) n=2 (B) n≥2, (C)
713 n≥3, (D) n≥3. *** p<0.001, ** p<0.01, *p<0.05.
714
715 **Figure 3: Elevated ISGylation in USP18$^{-/-}$ coincides with increased resistance to MHV-3**
716 **infection *in vitro*.**
717 (A) USP18$^{-/-}$ primary hepatocytes are more resistant to MHV-3 infection than USP18$^{+/+}$ mice.
718 Primary hepatocytes were infected with MHV-3 (MOI=1) and viral titers were assayed using a
719 standard plaque assay. Titering was represented by mean ± SD. n=3. (B) Elevated ISGylation
720 coincides with decreased N protein production in USP18$^{-/-}$ hepatocytes. Time course of N protein
721 production and ISG15 conjugate formation by WB. Hepatocytes were inoculated with MOI=1
722 and harvested at the indicated time points. N protein production is a marker of viral replication.
723 WB is a representative blot of two independent experiments. *** p<0.001, ** p<0.01, *p<0.05.
724
725 **Figure 4: ISGylation inhibits MHV-3 replication**
726 The E1 conjugation enzyme, Ube1L, is critical for ISG15 conjugation to target proteins. Ube1L
727 expression was silenced to determine if increased expression of ISG15 or increased ISGylation is
728 antiviral to coronavirus. Primary hepatocytes were transfected with Ube1L or control siRNA
729 (Santa Cruz) and incubated for 24h. Hepatocytes were infected with MHV-3 (MOI=1) and cells
730 were harvested 12h p.i.. Samples were visualized on a WB for Ube1L expression, N protein pro-
731 duction and ISGylation. Blot is representative of two independent experiments.
732

733 **Figure 5: PLP2 inhibitors and ISG15 antiviral activity inhibit MHV-3 N protein produc-**
734 **tion.**
735 PEM from USP18$^{+/+}$ or USP18$^{-/-}$ mice were inoculated with MHV-3 (MOI=0.1) for 1h, the virus
736 was then washed away and PEM were treated with PLP2 inhibitors (100µM inhibitor 6, 7 or
737 GRL0617) or IFN-α (100IU/ml) (34). Cells were harvested 9h p.i.. N protein and ISG15 conju-
738 gates were visualized by WB.
739
740 **Figure 6: ISGylation delays MHV-3 replication**
741 Increased ISGylation coincides with prolonged survival and delayed N protein accumulation.
742 USP18$^{+/+}$ or USP18$^{-/-}$ mice were infected with 50 PFU MHV-3/mouse. Mice (n=4) from each
743 group were sacrificed daily and livers were harvested for WB analysis. N protein and ISG15 con-
744 jugates were visualized by WB.
745
746 **Figure 7: The onset of PLP2 expression is delayed in USP18$^{-/-}$ mice**
747 N protein expression coincides with increased viral expression. To determine if PLP2 expression
748 followed this expression pattern we tested mRNA expression of PLP2 following MHV-3 expres-
749 sion. USP18$^{+/+}$ or USP18$^{-/-}$ mice (n=4/group) were infected with MHV-3 (50 PFU MHV-
750 3/mouse). Livers were harvested on the indicted days and mRNA was extracted. Data is repre-
751 sented as the fold increase of PLP2 mRNA over the housekeeping gene GAPDH. *** $p<0.001$.
752

Figure 1

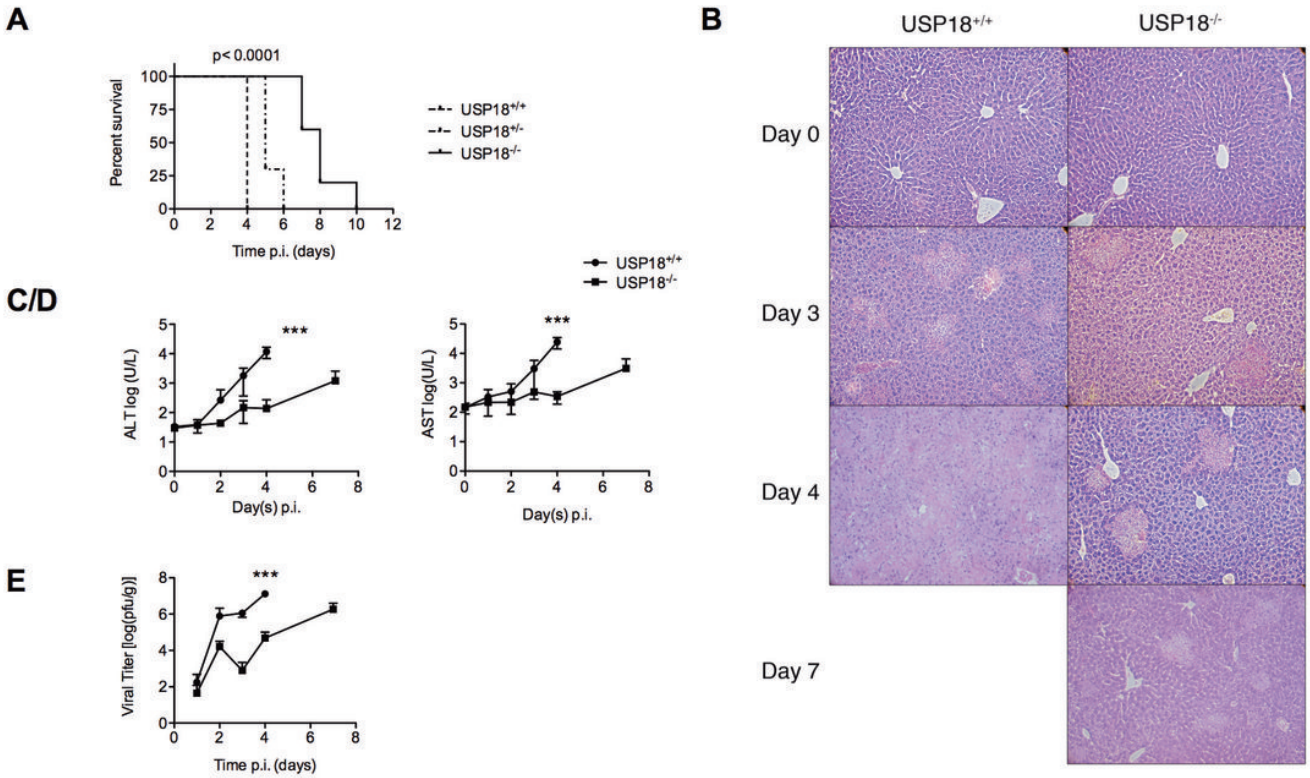

Figure 2

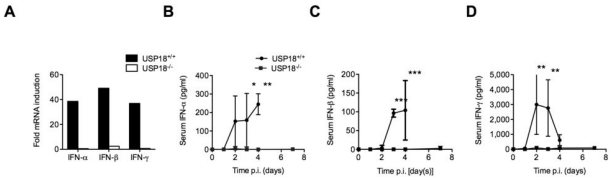

Figure 3

A

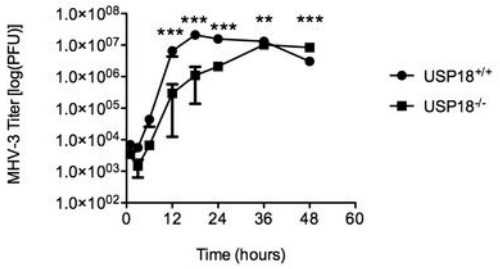

B

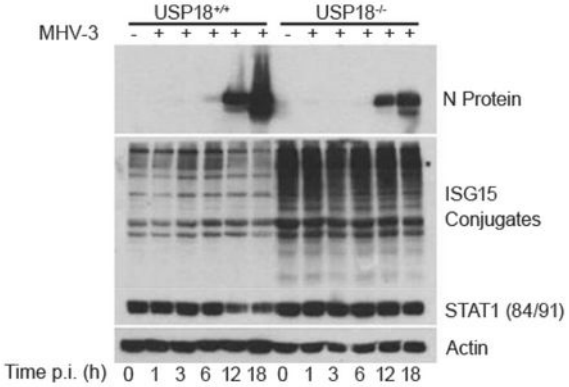

Figure 4

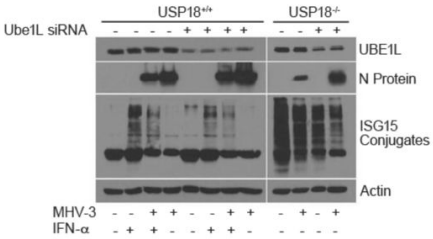

Figure 5

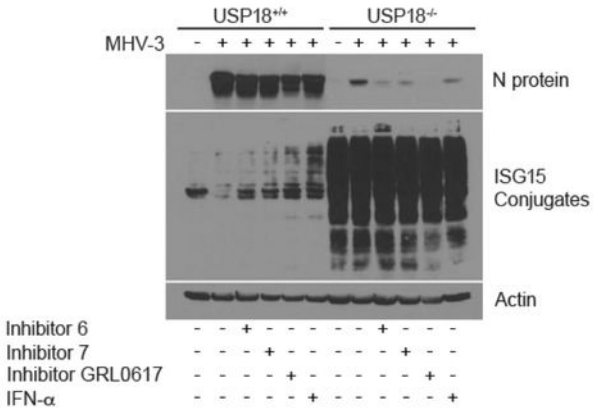

Figure 6

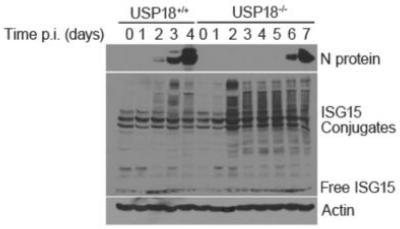

Figure 7